Methods 148 (2018) 4–8

Contents lists available at ScienceDirect

Methods

journal homepage: www.elsevier.com/locate/ymeth

Determination of the conformational states of strychnine in solution using NMR residual dipolar couplings in a tensor-free approach

Giulia Tomba, Carlo Camilloni[1], Michele Vendruscolo*

Department of Chemistry, University of Cambridge, Cambridge CB2 1EW, United Kingdom

A B S T R A C T

Small molecules with rotatable bonds can occupy different conformational states in solution as a consequence of their thermal fluctuations. The accurate determination of the structures of such states, as well as of their statistical weights, has been challenging because of the technical difficulties in extracting information from experimental measurements, which are normally averaged over the conformational space available. Here, to achieve this objective, we present an approach based on a recently proposed tensor-free method for incorporating NMR residual dipolar couplings as structural restraints in replica-averaged molecular dynamics simulations. This approach enables the information provided by the experimental data to be used in the spirit of the maximum entropy principle to determine the structural ensembles of small molecules. Furthermore, in order to enhance the sampling of the conformational space we incorporated the metadynamics method in the simulations. We illustrate the method in the case of strychnine, determining the three major conformational states of this small molecule and their associated occupation probabilities.

1. Introduction

The determination of the conformational states of small molecules in solution is an important but challenging problem in structural biology and medicinal chemistry [1–4]. While the binding affinity between molecular partners depends quite strongly on their structural compatibility, it is well known that molecular structures are not fixed but rather undergo conformational fluctuations that reflect their underlying free energy landscape [5–9]. Since even small conformational changes can result in large differences in establishing successful ligand-receptor interactions, achieving high accuracy in determining the accessible conformational space is paramount [2,10].

Nuclear magnetic resonance (NMR) spectroscopy offers an arsenal of powerful methods for studying the structure and dynamics of molecules in solution. In recent years, the use of NMR residual dipolar couplings (RDCs) to investigate the structure and dynamics of small organic molecules has gained increasing popularity [11–15]. As already well established for proteins and nucleic acids [16–20], RDCs offer detailed structural and dynamical information on time scales up to the millisecond time scale. Standard interpretations of RDCs are based on the introduction of an alignment tensor to describe the preferential orientation of the molecule under investigation with respect to the alignment medium [21,22]. The alignment tensor can be determined via fitting procedures to experimental data such as the singular-value decomposition (SVD) method [23] or via structure-based approaches [24–26]. For rigid molecules, the former approach is quite effective. However, for certain electrostatic alignment media and when conformational fluctuations are relatively large, fitting procedures are at risk of inaccuracy [20,27,26] and structure-based methods can be more effective [28,26,20]. These methods, however, become problematic in the presence of conformational fluctuations.

To overcome these limitations, a tensor-free strategy has been recently proposed and shown to provide accurate simultaneous determination of the structure and dynamics of proteins [29,30]. In order to implement this strategy the conformational sampling can be conveniently provided by all-atom molecular dynamics simulations [31–33]. As shown for biomolecules [34–37], a particularly powerful strategy to implement these simulations is to use the experimental data themselves to bias the sampling of the conformational space. In this case, the data are used as replica-averaged structural restraints so that the force-field used in the simulation is corrected and brought to match the experimental data according to the maximum entropy principle [38,39].

We provide here initial evidence for the utility of this approach for the conformational analysis of small organic molecules by studying the free energy landscape of strychnine, a toxic alkaloid with a complex conformational space. Strychnine has been commonly assumed to populate a well-defined structure and extensively used as a test molecule for NMR measurements and in the development of alignment media for organic solvents. Recent studies, however, have challenged this view

* Corresponding author.
E-mail address: mv245@cam.ac.uk (M. Vendruscolo).
[1] Current address: Dipartimento di Bioscienze, Universita' degli studi di Milano, Milano, Italy.

https://doi.org/10.1016/j.ymeth.2018.07.005
Received 22 March 2018; Received in revised form 10 July 2018; Accepted 17 July 2018
Available online 21 July 2018
1046-2023/

and proposed that elusive conformational transitions may be present [40–42]. The analysis that we present here adds further insight into this question and indicates the possibility of identifying the presence of conformers with low populations.

2. Methods

The molecular dynamics simulations were run in GROMACS 4.6.5 [43] using PLUMED 2.1 [44]. OPLS/AA [45] parameters for strychnine were derived using the ACPYPE tool [46]. We adopted the topology for a rigid model of the solvent molecule $CHCl_3$ uploaded to the GROMACS website by PeiQuan Chen in 2013. The computed density of a 512-molecule solvent box at the temperature of 300 K and pressure of 1 bar was 1.458 g/cm^3 for this model (to be compared with an experimental value 1.473 g/cm^3 [47]). Non-bonded interactions needed to be implemented with a cutoff of 1.4 nm to ensure such agreement.

A time step of 2 fs was used together with LINCS constraints [48]. All simulations were carried out in the canonical ensemble at constant volume and by thermosetting the system with the Nosé-Hoover thermostat [49].

The starting conformation of strychnine was taken from an X-ray crystal structure (PDB code 2XYS) code 2XYS) and solvated with 230 $CHCl_3$ molecules in a cubic box of volume 32 nm^3. A preliminary simulation of over 100 ns at 300 K yielded a trajectory for the analysis of the degrees of freedom of the solute in order to choose the collective variables for the metadynamics approach (see below). A comprehensive analysis of the distribution for all dihedral angles highlighted a more or less pronounced bimodal distribution in a number of cases, which translated into a flexibility of the inner rings (in particular C, D, F, G, see Fig. 1). Among this subset, we selected five independent dihedral angles to be used to enhance the sampling in the molecular dynamics simulations. This enhanced sampling was implemented using replica-averaged metadynamics (RAM) simulations [50], which we performed using NMR residual dipolar couplings (RDCs) as replica-averaged restraints [51,25,26,20] and bias-exchange metadynamics [52].

According to the bias-exchange metadynamics approach, which combines replica exchange [53] with metadynamics [54,55], several metadynamics simulations are performed in parallel on different replicas of the system, each replica biasing a different collective variable (CV). Exchanges between the replicas are attempted periodically according to a replica-exchange scheme. The choice of the collective variables is crucial for the success of the metadynamics approach. Here, we focused on torsional angles related to the flexibility of the inner rings of strychnine. Our setup comprised eight replicas of the system, five of which were biased each along one of the following torsion angles (see Fig. 1: $C13{-}O25{-}C24{-}C23$ (CV1), $C17{-}C7{-}C18{-}C19$ (CV2), $C16{-}C17{-}N20{-}C21$ (CV3), $C10{-}C12{-}C13{-}C14$ (CV4) and $C15{-}C22{-}C23{-}C24$ (CV5)). No bias was applied on the remaining three replicas. Gaussians were deposited every 500 steps with $\sigma = 0.1$ nm. The initial height of the Gaussians (0.5 kJ/mol) was rescaled according to the well-tempered scheme [56] with a bias-factor of 12 to improve the convergence of the simulations. Exchanges between the replicas were attempted every 50 ps. Each replica was simulated for at least 130 ns. The convergence of the sampling was assessed by monitoring the differences of the free energies at successive points of the simulation and was well reached within 60 ns simulated time. The sampling of the eight replicas was used to generate a five-dimensional CV-space into a homogeneous grid of small hypercubes whose free energies were obtained using a standard weighted histogram analysis [57–60]. Uncertainties on the free energy of the different states (as derived by WHAM [61]) were propagated up to the population analysis using standard error propagation rules.

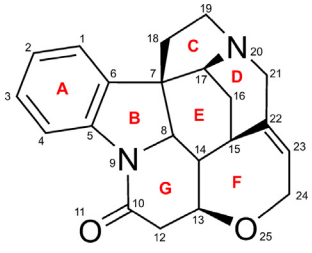

Fig. 1. Schematic of strychnine.

We considered two different sets of experimental RDCs available in the literature to be used as structural restraints in the RAM simulations. The first one (referred to as “set1” hereafter), obtained by Luy et al. [62,63] for strychnine in stretched polystyrene (PS)/$CDCl_3$ gel at 300 K, comprises 19 D_{CH} values. The second one (“set2”), was measured by Thiele et al. [64] for strychnine in PELG/$CDCl_3$ at 300 K and used as reference in further recent analysis [40]. This set includes three more D_{CH} values (C3H3, C18H181 and C18H182), for a total of 22. The RDC data were incorporated as replica-averaged structural restraints following the recently developed θ method [29,30], where the role of the structural restraint is to minimize the deviation between the value of the angle θ derived from the measured RDC and that calculated in the refinement protocol for every pair of nuclei for which an RDC value is available from the experiment. We first restrained the correlation between the experimental and calculated RDCs using a large force constant until we obtained a value of ~1 [29]. This allowed us to calculate the effective scaling factor using a linear fit of the experimental and calculated RDCs. Thereafter, the Q-factor was restrained to ~0 using this optimized scaling factor and an optimized force constant value (8000 kJ/mol) to sample the conformational space compatible with the averaged restraints and thus generate an ensemble of conformations consistent with the RDCs. A further, unrestrained (“free”) simulation was run under the same identical bias-exchange setup in order to compare the results obtained purely on the basis of the OPLS force-field. Lastly, three more simulations (restrained according to set1, restrained according to set2, free) were performed for strychnine in water (TIP4P model [65]) to assess the influence of the solvent in the simulation. In this case, the cutoff of the non-bonded interactions was set to 0.9 nm, while all the other parameters were the same as for the simulations in chloroform.

3. Results and discussion

Our simulations enabled us to obtain free energy profiles of the collective variables (CVs) used to enhance the sampling (see Methods). These free energy profiles, together with the corresponding two-dimensional free energy landscapes (Fig. 3), revealed three torsion angles that assume two different values (Fig. 2). The analysis of the free energy profiles for these CVs, extracted at successive time points of the simulations, also confirmed the convergence of the simulations (Fig. 2). The simulation restrained with set1 is taken here as representative case. Only one minimum was found for both CV4 and CV5, so their contribution to the description of the system can be considered as negligible. As a consequence, we reduced the five-dimensional free energy landscape to three dimensions for further analysis, and in particular for the search of local minima that could be identified as significant conformers.

As shown in Fig. 3, the vast majority of the structures obtained from the simulations (94.9% of the total population in the set1-restrained simulation) could be grouped into a conformer labelled here as A. However, at variance with what one would expect for a completely rigid molecule, a significant part of the overall population (4.9%) could be identified as a different conformer B, while a third, faint minimum identified a third, less populated conformer C (0.2%). Conformer B mainly differs from conformer A by buckling of the C-ring. Conformer C differs more pronouncedly through a distorsion of the 7-membered F-ring, which is no longer in chair conformation (“oxygen-up”) but rather in an envelope conformation (“oxygen-down”).

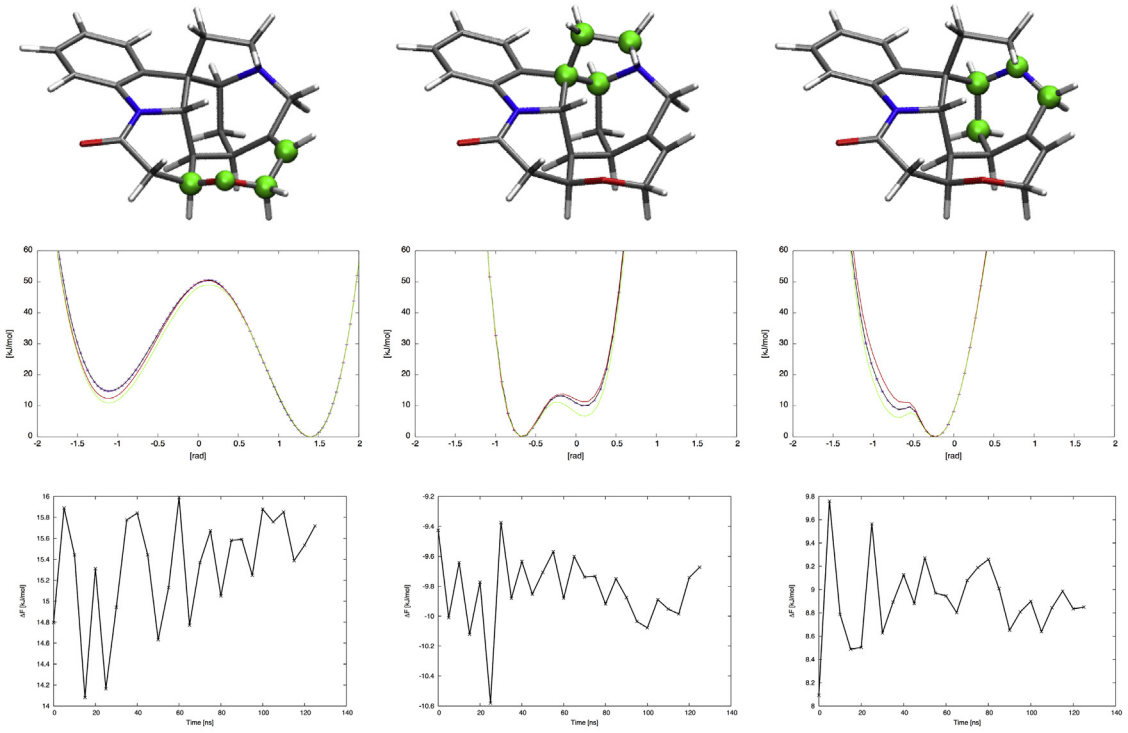

Fig. 2. Our simulations revealed three torsion angles that assume two distinct values. The convergence of the simulations was assessed by the free energy profiles for the three most relevant CVs used during the simulation (atoms identifying the corresponding dihedrals are highlighted in green in the structures on top). We show the profiles for the simulation restrained with set1 (black, averaged over the final 50 ns of the simulation, with red error bars reporting the standard deviation), with set2 (red), free (green). For further evaluation of the convergence, plots on the bottom line show the corresponding free-energy differences between the two local minima as a function of simulated time (set1 is reported as example). (For interpretation of the references to colour in this figure legend, the reader is referred to the web version of this article.)

As shown in Table 1, the use of the more complete set2 as RDC restraints led to a slight redistribution in the populations, with %B and %C being slightly increased. Of the three more values present in set2 with respect to set1, two refer to the C-ring of strychnine (C18 and its two diastereotopic protons), and can well influence the behaviour of the molecule, thus explaining the small difference between the two results. When compared with the free (unrestrained) simulation, it becomes clear that both sets of experimental data work towards stiffening

Table 1
Populations and relative uncertainties (in %) of states A, B and C of strychnine for the simulations in chloroform at 300 K.

	A	B	C
set1	94.90 ± 0.15	4.90 ± 0.12	0.20 ± 0.01
set2	91.76 ± 0.19	6.50 ± 0.11	1.74 ± 0.05
free	87.97 ± 0.28	11.18 ± 0.21	0.85 ± 0.03

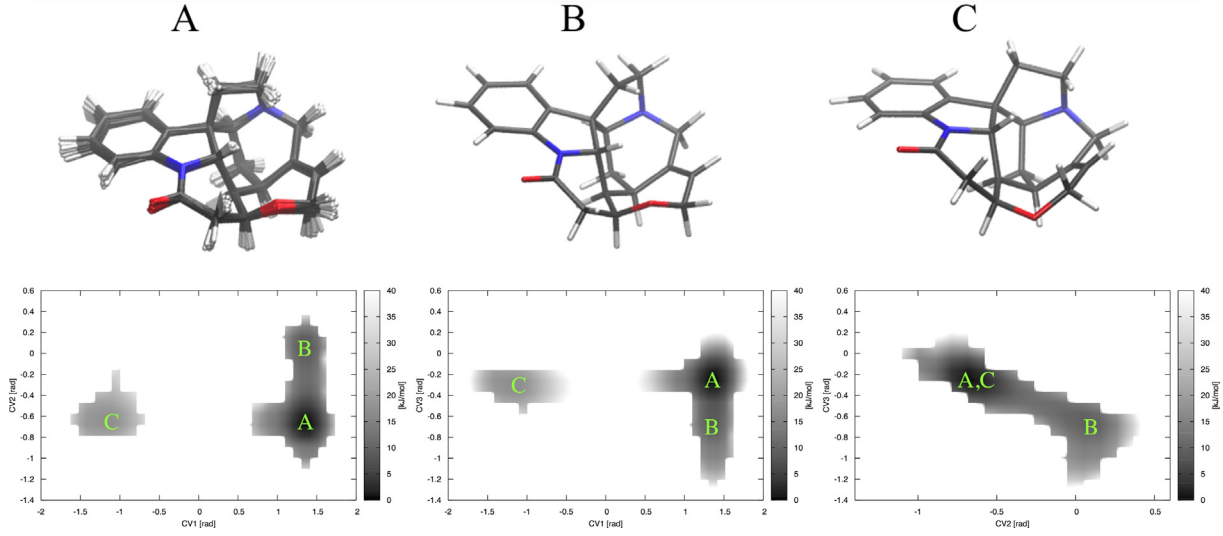

Fig. 3. The two-dimensional free energy landscapes obtained from the simulation restrained with set1 show three local minima corresponding to three different conformers A, B, C depicted above (see Supplementary Data). A: CV1 = 1.41, CV2 = −0.68, CV3 = −0.26; B: CV1 = 1.31, CV2 = 0.05, CV3 = −0.68; C: CV1 = −1.2, CV2 = −0.68, CV3 = −0.26.

Table 2
Populations and relative uncertainties (in %) of states A, B and C of strychnine for the simulations in water at 300 K.

	A	B	C
set1	94.42 ± 0.14	4.32 ± 0.10	1.26 ± 0.04
set2	97.63 ± 0.05	2.09 ± 0.04	0.28 ± 0.01
free	84.29 ± 0.35	9.13 ± 0.19	6.58 ± 0.21

the C-ring of the molecule with respect to the OPLS force-field alone, which significantly overestimated the B population. The correction given by the experimental data to the force-field is even more crucial than in the case of biomolecules, since parametrization of organic compounds has often not kept the pace in terms of accuracy with that of proteins and nucleic acids, despite recent improvements [66–68,46].

It may be of interest to know whether the use of RDC restraints leads to the same populations even for simulations performed in water rather than in the solvent used for the RDC measurements, since water models are far more available and better tested for compatibility with a wide range of force-fields than organic solvents, so their use may prove easier in further work. A simulation in water with no corrections on the force-field deviated significantly from the analogous one in chloroform, yielding a large overestimation of population C (see Table 2). On the other side, the two RDC-restrained simulations were both successful in bringing the population values closer to what obtained in chloroform.

In order to assess the quality of the ensembles of structures obtained from our simulations, we calculated the quality factors Q [69] for the RDCs used as restraints, using the standard SVD to back-calculate the RDCs from subsets of 6000 structures. As shown in Table 3, the use of the RDC restraints brought significant improvement in the overall quality of the structures with respect to the "free" simulations. Better results for the RDC set1 suggest that set2 may be affected by larger experimental errors.

We also carried out a further validation using distances between hydrogen atom pairs derived from NOE measurements [70]. More specifically, we compared the agreement between NOE-derived distances and the corresponding distances calculated from the simulations (Fig. 4). As expected, we found that for both set1 and set2, the agreement improved with respect to the unrestrained (free) simulations, although only slightly. These results are encouraging and, together with those reported above about the influence of the force field and of the number of RDCs used in the simulations on the populations of the different states of strychnine, indicate that the use of more accurate force fields and additional RDC data within the tensor-free approach that we have introduced in this work may enable the populations of the different states of strychnine to be estimated to within 1% accuracy, which we believe will be an achievable target in future studies.

The results presented so far indicate that the traditional characterisation of strychnine as a highly rigid molecule is not completely accurate. Indeed, this more dynamic view of strychnine has been recently put forward by other authors. A possible buckling of the C-ring was recently mentioned by Bifulco et al. [42], who took into consideration a higher-energy conformer for strychnine (very similar to B) derived from quantum–mechanical calculations, but estimated it to contribute very little to the conformational equilibrium at room temperature (0.11%). The existence of a conformer largely similar to the representative structure of basin C was recently revealed in two publications and hailed as the evidence of a hidden flexibility of the molecule. In these studies, Schmidt et al. [40] presented experimental and DFT-level theoretical evidence suggesting a population for the minority conformer of 2.7% and 1.9% at 298 K, respectively. Butts et al. [41] proposed a population for the same conformer of 1–2% at 298 K, based again on DFT-level calculations.

Most studies based on RDC data published so far for strychnine limited their analyses to the use of a single alignment tensor [71,64]. Schmidt et al. [40] fitted the RDC data using two conformers (A and C). As this procedure resulted in an unlikely 87:13 ratio, they concluded that an RDC analysis, while hinting correctly to the existence of conformational averaging, is not precise enough to determine the populations with sufficient precision. A similar consideration was made in a study by Thiele et al. [72] on α-methylene-γ-butyrolactone, which concluded that RDCs can only determine conformer populations with a precision of about 7%. Recently, another paper by Thiele et al. [70] aimed to sum up the information provided by NOE and RDC measurements for strychnine and concluded that the experimental data could be best fitted by admitting the existence of flexibility in the F-ring (with a 2% population for what we call here conformer C) but no flexibility in the C-ring (our conformer B). These results, together with those that we obtained in the present studies using simulations in two different solvents and two different RDC datasets, indicate again that more accurate force fields and more extensive experimental data will be needed to determine with high accuracy the populations of the different conformers. In this context, the tensor-free method that we describe in this work provides an effective solution to the problem of representing the dynamics of small molecules by calculating accurately the populations of the different states that they occupy, which previously has been approached using more complex approaches such as the multiple tensor analysis applied by Thiele et al. to the case of α-methylene-γ-butyrolactone [72].

Table 3
Assessment of the quality of the structural ensembles obtained in chloroform and water using set1, set2 or no RDC restraint. In each case, we report the Q factor calculated with respect to the RDC set1 [63] and the RDC set2 [64] (first and second number, respectively).

Chloroform			Water		
set1	set2	free	set1	set2	free
0.10/0.14	0.11/0.13	0.13/0.16	0.10/0.14	0.12/0.12	0.15/0.16

4. Conclusions

We have presented a strategy for using RDCs as tensor-free structural restraints in replica-averaged molecular dynamics simulations to determine the conformations accessible to a small molecule, together with their corresponding statistical weights. The application of this strategy to strychnine has enabled us to rationalise the lack of consensus in the literature regarding the existence of several conformers for this small molecule. The observation that some of its conformational states are so low-populated contributes to the difficulty in obtaining conclusive results based on quantum-mechanical calculations alone. On the other side, the high risk of inaccuracy for fitting-based procedures when different conformers are present may explain why they miss to detect very low-populated states. We have shown that our approach can offer a way to overcome these problems and to quantify the conformer populations of strychnine with high accuracy, in particular in conjunction with more accurate force fields.

We anticipate that this method will be readily applicable to determining the conformational states of any other organic molecule for which high-quality RDC data are available. We believe that application to small molecule drug candidates may lead to important insights for their design, both in terms of improving their effectiveness and of avoiding potential toxic effects.

Appendix A. Supplementary data

Supplementary data associated with this article can be found, in the online version, at https://doi.org/10.1016/j.ymeth.2018.07.005.

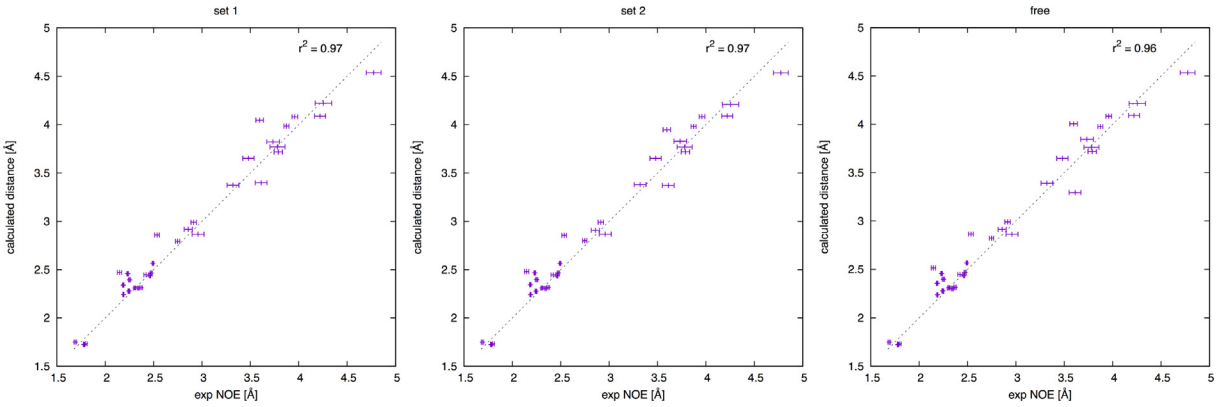

Fig. 4. Comparison of interproton distances determined by NOE measurements [70] and by Boltzmann averaging of the three conformers in the simulations restrained with set1 and set2, and in the free simulations.

References

[1] R. Baron, J.A. McCammon, Annu. Rev. Phys. Chem. 64 (2013) 151–175.
[2] D.D. Boehr, R. Nussinov, P.E. Wright, Nat. Chem. Biol. 5 (2009) 789–796.
[3] D.L. Mobley, K.A. Dill, Structure 17 (2009) 489–498.
[4] P. Pisani, P. Piro, S. Decherchi, G. Bottegoni, D. Sona, V. Murino, W. Rocchia, A. Cavalli, J. Chem. Theory Comput. 10 (2014) 2557–2568.
[5] H. Frauenfelder, S.G. Sligar, P.G. Wolynes, Science 254 (1991) 1598–1603.
[6] J.N. Onuchic, Z. Luthey-Schulten, P.G. Wolynes, Annu. Rev. Phys. Chem. 48 (1997) 545–600.
[7] K. Henzler-Wildman, D. Kern, Nature 450 (2007) 964.
[8] K. Lindorff-Larsen, R.B. Best, M.A. DePristo, C.M. Dobson, M. Vendruscolo, Nature 433 (2005) 128.
[9] M. Bonomi, G.T. Heller, C. Camilloni, M. Vendruscolo, Curr. Opin. Struct. Biol. 42 (2017) 106–116.
[10] C.E. Tinberg, S.D. Khare, J. Dou, L. Doyle, J.W. Nelson, A. Schena, W. Jankowski, C.G. Kalodimos, K. Johnsson, B.L. Stoddard, D. Baker, Nature 501 (2013) 212.
[11] C.M. Thiele, A. Marx, R. Berger, J. Fischer, M. Biel, A. Giannis, Angew. Chem. Int. Ed. 45 (2006) 4455–4460.
[12] C.M. Thiele, Eur. J. Org. Chem. (2008) 5673–5685.
[13] C. Farès, J. Hassfeld, D. Menche, T. Carlomagno, Angew. Chem. Int. Ed. 47 (2008) 3722–3726.
[14] G. Kummerlöwe, B. Luy, Trends Anal. Chem. 28 (2009) 483–493.
[15] G. Kummerlöwe, B. Crone, M. Kretschmer, S.F. Kirsch, B. Luy, Angew. Chem. Int. Ed. 50 (2011) 2643–2645.
[16] J.H. Prestegard, C.M. Bougault, A.I. Kishore, Chem. Rev. 104 (2004) 3519–3540.
[17] J.-C. Hus, D. Marion, M. Blackledge, J. Am. Chem. Soc. 123 (2001) 1541–1542.
[18] P. Bayer, L. Varani, G. Varani, J. Biomol. NMR 14 (1999) 149–155.
[19] O.F. Lange, N.-A. Lakomek, C. Farès, G.F. Schröder, K.F.A. Walter, S. Becker, J. Meiler, H. Grubmüller, C. Griesinger, B.L. de Groot, Science 320 (2008) 1471–1475.
[20] A. De Simone, R.W. Montalvao, C.M. Dobson, M. Vendruscolo, Biochemistry 52 (2013) 6480–6486.
[21] N. Tjandra, A. Bax, Science 278 (1997) 1111–1114.
[22] A. Saupe, G. Englert, Phys. Rev. Lett. 11 (1963) 462–464.
[23] J.A. Losonczi, M. Andrec, M.W.F. Fischer, J.H. Prestegard, J. Magn. Reson. 138 (1999) 334–342.
[24] M. Zweckstetter, A. Bax, Nat. Protoc. 3 (2000) 679–690.
[25] A. De Simone, R.W. Montalvao, M. Vendruscolo, J. Chem. Theory Comput. 7 (2011) 4189–4195.
[26] R.W. Montalvao, A. De Simone, M. Vendruscolo, J. Biomol. NMR 53 (2012) 281–292.
[27] A. De Simone, M. Gustavsson, R.W. Montalvao, L. Shi, G. Veglia, M. Vendruscolo, Biochemistry 52 (2013) 6684–6694.
[28] M. Louhivuori, K. Paakkonen, K. Fredriksson, P. Permi, J. Lounila, A. Annila, J. Am. Chem. Soc. 125 (2003) 15647–15650.
[29] C. Camilloni, M. Vendruscolo, J. Phys. Chem. B 119 (2015) 653–661.
[30] R.W. Montalvao, C. Camilloni, A. De Simone, M. Vendruscolo, J. Biomol. NMR 58 (2014) 233–238.
[31] W.L. Jorgensen, Science 303 (2004) 1813–1818.
[32] E.H. Lee, J. Hsin, M. Sotomayor, G. Comellas, K. Schulten, Structure 17 (2009) 1295–1306.
[33] R.O. Dror, R.M. Dirks, J. Grossman, H. Xu, D.E. Shaw, Ann. Rev. Biophys. 41 (2012) 429–452.
[34] R.B. Best, M. Vendruscolo, J. Am. Chem. Soc. 126 (2004) 8090–8091.
[35] K. Lindorff-Larsen, R.B. Best, M.A. DePristo, C.M. Dobson, M. Vendruscolo, Nature 433 (2005) 128–132.
[36] M. Vendruscolo, Curr. Opin. Struct. Biol. 17 (2007) 15–20.
[37] J. Huang, S. Grzesiek, J. Am. Chem. Soc. 132 (2010) 694–705.
[38] J.W. Pitera, J.D. Chodera, J. Chem. Theory Comput. 8 (2012) 3445–3451.
[39] A. Cavalli, C. Camilloni, M. Vendruscolo, J. Chem. Phys. 138 (2013) 094112.
[40] M. Schmidt, F. Reinscheid, H. Sun, H. Abromeit, G.K.E. Scriba, F.D. Sönnichsen, M. John, U.M. Reinscheid, Eur. J. Org. Chem. (2014) 1147–1150.
[41] C.P. Butts, C.R. Jones, J.N. Harvey, Chem. Commun. 47 (2011) 1193–1195.
[42] G. Bifulco, R. Riccio, G.E. Martin, A.V. Buevich, R.T. Williamson, Org. Lett. 15 (2013) 654–657.
[43] S. Pronk, S. Pall, R. Schulz, P. Larsson, P. Bjelkmar, R. Apostolov, M.R. Shirts, J.C. Smith, P.M. Kasson, D. van der Spoel, B. Hess, E. Lindahl, Bioinformatics 29 (2013) 845–854.
[44] G.A. Tribello, M. Bonomi, D. Branduardi, C. Camilloni, G. Bussi, Comput. Phys. Commun. 185 (2014) 604–613.
[45] W.L. Jorgensen, D.S. Maxwell, J. Tirado-Rives, J. Am. Chem. Soc. 118 (1996) 11225–11236.
[46] A.W.S.D. Silva, W.F. Vranken, BMC Res. Notes 5 (2012) 367.
[47] R.C. Weast, Handbook of Chemistry and Physics, CRC Press, 1988.
[48] B. Hess, J. Chem. Theory Comput. 4 (2008) 116–122.
[49] D.J. Evans, B.L. Holian, J. Chem. Phys. 83 (1985) 4069–4074.
[50] C. Camilloni, A. Cavalli, M. Vendruscolo, J. Chem. Theory Comput. 9 (2013) 5610–5617.
[51] A. De Simone, B. Richter, X. Salvatella, M. Vendruscolo, J. Am. Chem. Soc. 131 (2009) 3810–3811.
[52] S. Piana, A. Laio, J. Phys. Chem. B 111 (2007) 4553–4559.
[53] Y. Sugita, Y. Okamoto, Chem. Phys. Lett. 314 (1999) 141–151.
[54] A. Laio, F.L. Gervasio, Rep. Prog. Phys. 71 (2008) 126601-1–126601-22.
[55] A. Laio, M. Parrinello, Proc. Nat. Acad. Sci. 99 (2002) 12562–12566.
[56] A. Barducci, G. Bussi, M. Parrinello, Phys. Rev. Lett. 100 (2008) 020603/1–020603/4.
[57] F. Marinelli, F. Pietrucci, A. Laio, S. Piana, PLoS Comput. Biol. 5 (2009) e1000452.
[58] D. Granata, C. Camilloni, M. Vendruscolo, A. Laio, Proc. Nat. Acad. Sci. 110 (2013) 6817–6822.
[59] F. Baftizadeh, P. Cossio, F. Pietrucci, A. Laio, Curr. Phys. Chem. (2012) 2.
[60] X. Biarnes, F. Pietrucci, F. Marinelli, A. Laio, Comput. Phys. Commun. 183 (2012) 203–211.
[61] S. Kumar, D. Bouzida, R.H. Swendsen, P.A. Kollman, J.M. Rosenberg, J. Comput. Chem. 13 (1992) 1011–1021.
[62] B. Luy, K. Kobzar, H. Kessler, Angew. Chem. Int. Ed. 43 (2004) 1092–1094.
[63] A.O. Frank, J.C. Freudenberger, A.K. Shaytan, H. Kessler, B. Luy, Magn. Reson. Chem. 53 (2015) 213–217.
[64] C.M. Thiele, J. Org. Chem. 69 (2004) 7403–7413.
[65] W.L. Jorgensen, J. Tirado-Rives, J. Am. Chem. Soc. 110 (1988) 1657–1666.
[66] F.-Y. Dupradeau, C. Cézard, R. Lelong, E. Stanislawiak, J. Pêcher, J.C. Delepine, P. Cieplak, Nucleic Acid Res. 36 (2008) D360–D367.
[67] F.-Y. Dupradeau, A. Pigache, T. Zaffran, C. Savineau, R. Lelong, N. Grivel, D. Lelong, W. Rosanski, P. Cieplak, PCCP 12 (2010) 7821–7839.
[68] K. Vanommeslaeghe, A.D. Mackerell Jr., J. Chem. Inf. Model. 52 (2012) 3144–3154.
[69] G. Cornilescu, J.L. Marquardt, M. Ottiger, A. Bax, J. Am. Chem. Soc. 120 (1998) 6836–6837.
[70] A. Kolmer, L.J. Edwards, I. Kuprov, C.M. Thiele, J. Magn. Reson. 261 (2015) 101–109.
[71] C.M. Thiele, S. Berger, Org. Lett. 5 (2003) 705–708.
[72] C.M. Thiele, V. Schmidts, B. Böttcher, I. Louzao, R. Berger, A. Maliniak, B. Stevensson, Angew. Chem. Int. Ed. 121 (2009) 6836–6840.